

The detection of bearing faults for induction motors by using vibration signals and machine learning

Eyüp Irgat, Eyüp Çınar, Abdurrahman Ünsal

Abstract -- Bearing faults are the most common type of faults in induction motors. Vibration monitoring is frequently employed to detect and diagnose these faults at their early stages. However, analysis of vibration signals most often requires expert knowledge and an in-depth understanding of specific tool mechanics. Recently, data-based modeling approaches coupled with machine learning algorithms gained significant attraction in the field, which can help manufacturers obtain faster and more scalable fault detection solutions. In this study, three-axis vibration signals of a healthy motor and a motor with inner-race and outer-race bearing faults are collected. Various statistical features belonging to each vibration axis are analyzed. The results show that among the statistical features extracted for each axis, peak-to-peak (p2p) and rms features of vibration signals are the most important features that can distinguish a healthy motor state from a faulty state; however further information is needed to be able to differentiate among faulty states. We have investigated various multi-axis statistical features and employed relatively two simple machine learning (ML) algorithms K-Nearest Neighbors (*k*-NN) and Decision Trees (DT) to obtain a model. Our results show that combined with ML models bearing faults can be distinguished with accuracies nearly up to 100 %.

Index Terms-- Machine Learning, Ball bearings, Induction motors, Vibration measurement, Condition monitoring

I. INTRODUCTION

Electric machines are widely used in all areas of applications with motion in the modern world. They consume most of the globally produced electricity and play a vital role in developing and automating modern industrial applications. Among the electric machines, induction motors are the most widely used ones in various applications due to their simple design, low cost, and higher efficiency [1, 2]. Widely usage of induction motors makes the maintenance and their healthy operations vital for many industries. In most applications, induction motors are used in heavy conditions and therefore are subject to various faults due to mechanical stress, thermal stress, and environmental conditions [3, 4]. Faults of an induction motor may lead to undesirable results such as failure of the production line, environmental damage, loss of life, process disruption, significant economic losses, unplanned stops, high maintenance costs. The faults of induction motors can be classified as electrical and mechanical faults. Electrical faults include rotor and stator faults, while mechanical faults include bearing faults, air gap eccentricity, and misalignment. The

bearing faults are accounted for 40% to 50% of total induction motor faults [5]. Two surveys conducted by the IEEE Industry Application Society (IEEE-IAS) and the Japan Electrical Manufacturers' Association (JEMA) show that bearing faults are responsible for 30% to 40% of all motor faults.

Monitoring, detection, and diagnosis of faults for induction motors, especially detection at early stages, are essential for all applications. Detection, diagnostics, and prognostics of motor faults at an early stage allow appropriately scheduled maintenance to prevent costly failures, avoid expensive economic losses, prevent unexpected downtime, and provide maximum tool uptime in production [6, 7]. Some motor faults, such as rotor faults, may even lead to a secondary fault in the motor. For example, a rotor with broken bars produces vibrations on the shaft, resulting in the eccentricity air gap, bearing faults, stator faults as a result of the rubbing of windings by broken rotor bars [3].

To prevent the undesirable results of faults, electrical motors are maintained periodically. However, the concept of conventional maintenance has been changed in parallel to the recent development of new technologies. The traditional forms of maintenance included both reactive and preventive approaches. In the reactive approach, also known as breakdown maintenance, no actions are taken to maintain equipment until it breaks and needs repair or replacement. In preventive maintenance approaches, periodic time-interval, regardless of the health condition of the equipment, is utilized to schedule maintenance. Reactive approaches might cause prolonged downtimes in manufacturing, and frequent preventive maintenance might cause unnecessary operational expenses. With the advancement of the Artificial Intelligence (AI) field and technologies, predictive maintenance (PdM) programs have drawn quite an interest among manufacturers [8]. A PdM program can be referred to as a condition-driven preventive maintenance program that consists of health assessment, diagnostics, and prognostics [9, 10]. The health assessment focuses on estimating and quantifying the health condition of the equipment. The diagnostics process is an automated fault detection system to detect faulty states and prognostics about forecasting equipment lifetime [11]. In a PdM program, the condition of the equipment is continuously monitored via signals without interrupting regular operation, and fault detection/prognosis operations are performed

This research was supported in part by the Scientific and Technical Research Council of Turkey (TUBITAK) under 2232 International Fellowship for Outstanding Researchers Program with grant number 118C252.

E. Irgat is with the Department of Kütahya Technical Sciences Vocational School, Kütahya Dumlupınar University, Germiyan Campus, 43020 Kütahya, Turkey (e-mail: eyup.ırgat@dpu.edu.tr).

E. Çınar is with the Department of Computer Engineering, Eskişehir Osmangazi University, Meşelik Campus, 26040 Eskişehir, Turkey (e-mail: eyup.cinar@rit.edu).

A. Ünsal is with the Department of Electrical Electronics Engineering, Kütahya Dumlupınar University, Evliya Çelebi Campus, 43100 Kütahya, Turkey (e-mail: unsal@dpu.edu.tr)

mainly utilizing data-based ML models. A PdM program can have a high return-on-investment (ROI) for manufacturers by reducing maintenance costs, losses and increasing the production capacity. It has been reported in [10] that a PdM program may reduce maintenance costs by 25% – 35%, eliminate equipment breakdowns by 70% – 75%, reduce downtime by 35% – 45% and consequently increase production capacity up to 25% – 35%.

The detection, diagnostics, and prognostics studies are conducted through knowledge of the changes occurring in the motor due to the faults. An expert might observe these changes utilizing some characteristic input signals or external sensors, including motor current, voltage, vibration, magnetic flux, temperature, and sound [12]. Among these signals, vibration monitoring is one of the most widely used for mechanical fault diagnosis for motor components.

Most of the conventional implementations of fault diagnosis of electrical machines are based on motor current signature analysis (MCSA) methods which are limited when the motor operates under different loads, different speeds, and different power ratings. These methods use the characteristic signal features of well-defined fault types which are not present at the early stage of a fault. Another limitation of these conventional methods arises when multiple faults with similar characteristic signal features are present simultaneously. In addition, the continuous monitoring of a system or mechanical equipment requires the recording, processing, transmission, and storing of a large amount of data.

For knowledge-based approaches, processing signals (current, voltage, vibration, sound, etc.) can be implemented in time-domain, frequency-domain, or time-frequency domain [13, 14]. Fast Fourier transform (FFT) [15], wavelet transformation (WT) [16], discrete wavelet transform [17], and wavelet packet transform (WPT) [18] are commonly used methods to transform vibration signals into frequency-domain for further processing and extraction of significant features for ML techniques. The frequency-domain methods effectively analyze stationary signals and are limited in the analysis of non-stationary signals. In addition, if the peak amplitude of the characteristic signals is not strong or the motor is lightly loaded, FFT-based methods may not be effective. In a WT, the selection of the suitable mother wavelet, the choice of decomposition level, and its frequency band require expert knowledge. On the other hand, in a time-domain analysis, looking at scalar indices such as peak value, peak-to-peak value, root-mean-square (RMS), and crest factor skewness, kurtosis, spectral kurtosis, impulse factor, shape factor, and clearance factor are suggested to determine the health state of induction motors [19]. The main disadvantage is the appropriate selection of the correct characteristic features to detect the faults.

To enhance the effectiveness of fault diagnosis and build a self-learning baseline model for various fault classes, data-based ML models can be utilized [20]. Artificial neural networks (ANN) [21], principal component analysis (PCA) [33], support vector machines (SVM) [22], k -NN [23], decision tree [24], and singular value decomposition (SVD)

[25] are among the well-known models for ML. Having a ML model that can learn from the data eliminates the development of complex physics-based fault detection models and prevents field engineers from adjusting alarm thresholds/rules for each equipment baseline in a fleet of similar equipment in the field.

Since nearly 50% of the inducting motor faults occur in bearing components [26], we have focused on experimentally investigating and validating the bearing-specific faults by utilizing vibration signals in a lab environment. The common single-row bearings with two rings, namely outer and inner rings, are used in induction motors. A set of rolling elements rotates between the two rings. Fig. 1 shows the main components of a single-row bearing [27]. The bearing faults may be caused due to wear and tear, aging, shock loads, overheating, imbalances, and improper lubrication [28, 29]. The common bearing faults appear in outer-race, inner-race, rolling element, and cage.

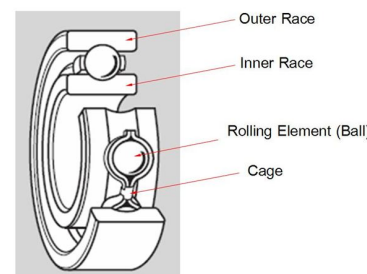


Fig. 1. Conceptual schematic showing the fundamental component details of a bearing [27]

The inner-race and outer-race faults of the bearings used in the study were implemented by drilling a hole on the inner and outer-race respectively. Fig. 2 shows fault-induced bearings. The motor is first tested with healthy bearings, followed by the bearing with inner-race fault and then with the bearing with outer race fault. The faulty bearings are mounted on the drive end of the induction motor.



Fig. 2. The bearings demonstrating the outer race fault (left) and the inner race fault (right)

The rest of the paper is organized as follows: first, the material and methods section is presented. In this section, we discuss how our experimental data from the testbed is collected and preprocessed together with the background behind artificially generated fault-induced scenarios. After this, experimental results obtained as a comprehensive analysis of vibration data descriptive statistics, and machine learning classification are presented. In the last section, we present discussions and conclusions from our experimental results for the reader.

II. MATERIAL AND METHODS

We utilize three-axis vibration signals to detect the inner-race and outer-race bearing faults of an induction motor. The vibration signals are first analyzed in the time domain by calculating peak-to-peak, rms, skewness, kurtosis, crest factor, and mean values. These values are used for feature extraction and classification. For classification, k -NN and DT methods are used to detect between healthy and faulty bearings, including the type of the bearing faults. The analysis of the motor's vibration signals with faulty bearings is compared to those of the motor with a healthy bearing. The accuracy rate of each method in detecting the healthy and faulty bearings is determined and compared with each other.

A. Data Collection

The dataset used in this study was recorded within a TUBITAK (The Scientific and Technological Research Council of Turkey) supported project with a grant number of 116E302. The schematic of the testbed is given in Fig. 3. It consists of a two-poles, 3-kW induction motor, a 5 kVA self-excited synchronous generator loaded with a variable resistive load, a 3-axis accelerometer (PCB356A31 with amplifier), and National Instrument (NI) data acquisition system (NI cDAQ 9174 with NI 9225 and NI 9227 modules). The vibration measurement axes are shown in Fig. 4. The vibration signals were recorded in three cases. In case 1, the motor was tested with an outer race faulty bearing. In case 2, the motor was tested with an inner-race faulty bearing. In case 3, the motor was tested with healthy bearings. The induction motor was loaded with 25%, 50%, 75%, and 100% of full load at each test case. At each test case and loading level, the NI data acquisition system recorded the three-axis vibration signals with a sampling frequency of 25 kHz and a length of 41 seconds. The rotor speed of the motor at full load was 2850 rpm. Each data set used in this study consists of 12 records grouped into four classes: four records of vibration signals with healthy bearing, four records of vibration signals with inner-race bearing fault, and four records of vibration signals with outer-race bearing faults.

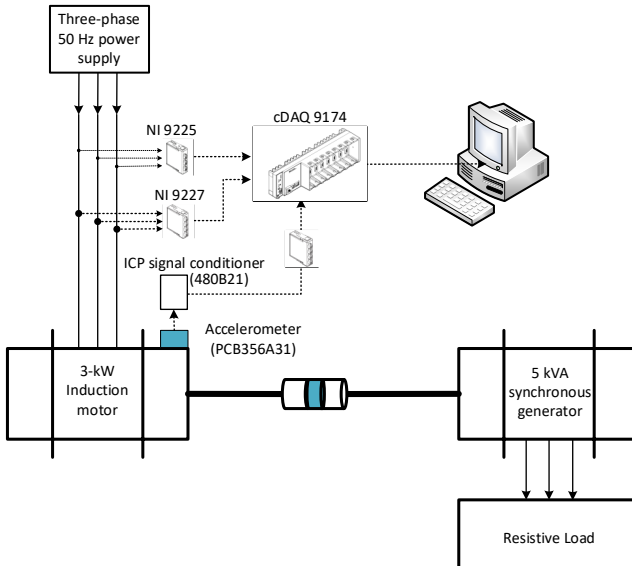


Fig. 3. Schematic of the testbed showing the individual hardware components where experimental vibration data is collected

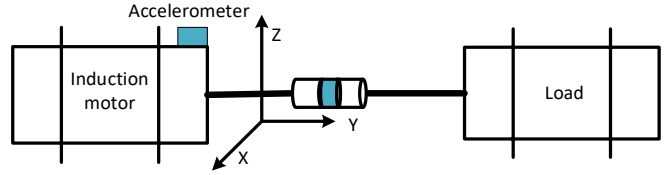


Fig. 4. Representative figure showing individual axis orientations for the accelerometer sensor placed on top of the induction motor

The raw vibration data collected from healthy bearing, inner race, and outer race faulty bearings while the motor is running at 100 % load level are plotted and shown in Fig. 5. The largest amplitudes of vibration are observed in z-axis signals, as shown in the bottom plot.

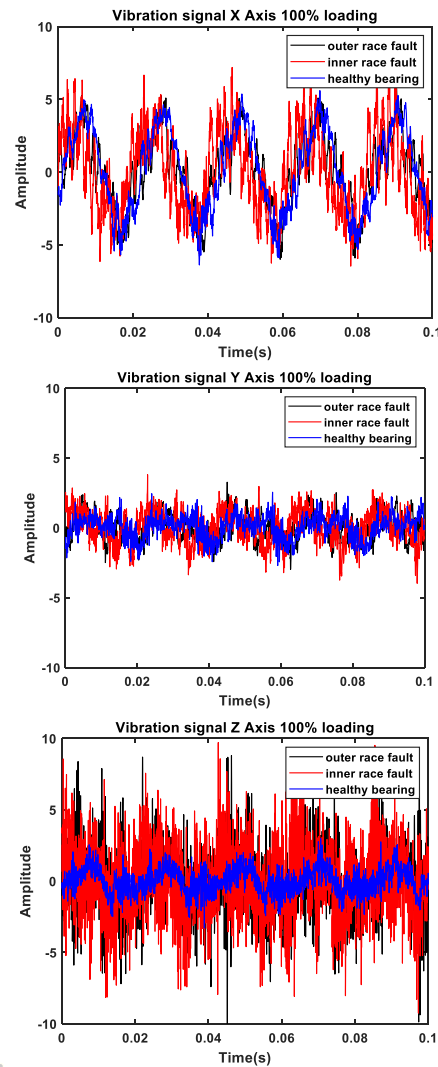


Fig. 5. Raw vibration data collected at 100 % load level from motors with a healthy bearing and bearings with outer/inner race faults

B. Preprocessing

The collected vibration data is first preprocessed in time-domain utilizing various statistical features on each vibration axis. These features include p2p, rms, skewness, kurtosis, crest factor, and mean values. The time window for each record is taken as 0.1 secs and selected statistical features are extracted for each time window. The whole dataset consists of 1230 rows for each loading level with data attributes for each axis's statistical features and corresponding classes such as healthy, outer, and inner faulty bearings.

C. Fault Classification via ML models

In this study, to obtain a self-learning fault diagnosis model for varying operational conditions and considering the experimental dataset and extracted features' aspects, rather simple supervised classification algorithms are preferred for our application. Thus, two classification algorithms, k -NN and DT classifiers, are employed.

The algorithm for k -nearest neighbor classification is a distance-based algorithm that computes distances (or similarity) between all training samples and the test sample. In the k -NN method, the nearest neighbors are measured with respect to k , which defines how many nearest neighbors need to be examined to describe the corresponding class of a test data point. The advantages of the k -NN method include simplicity, transparency, and rather less computational complexity that can be achieved with efficient indexing techniques to find nearest neighbors [30]. Each test data query is assigned to the class, represented by a majority of its k -nearest neighbors extracted from the entire training set by a selected distance metric.

The decision tree algorithm enables users to follow a tree structure to induct a decision. It is considered a relatively simple classifier method and yet widely used for classification tasks. The most important objective of a decision tree method is to extract a graph model by asking questions on select data attributes and split the tree into further branches for maximum information gain utilizing various impurity measures. Available decision tree construction algorithms utilized to grow trees are computationally inexpensive and thus give users an opportunity for higher efficiency and speed. Furthermore, the models obtained using DTs are more explainable and robust to noise in the dataset.

To optimize each algorithm's hyperparameters and obtain the highest model generalization performance, the k -fold cross-validation approach is employed on the experimental data.

III. RESULTS

After the extraction of statistical features from raw vibration signals for each axis, the box plots comparing the distribution of the parameters (peak-to-peak, rms, skewness, kurtosis, crest factor, and mean) belonging to the z -axis vibration are presented in Fig. 6. The vibration signals of healthy bearing, outer-race, and inner-race faulty bearings are presented only for the motor under 100% loading. Class 1 represents the outer-race faulty bearing, class 2 represents the inner-race faulty bearing, and class 3 represents the healthy bearing.

It is observed that p2p value belonging to inner-race faulty bearing, crest factor of both inner-race faulty bearing and healthy bearing, and kurtosis of healthy bearing have the most outliers. As expected, the rms and p2p values of the vibration signals of the healthy bearing are the lowest ones. The mean value for the healthy bearing is close to zero. The kurtosis values are around three, which means that the vibration signal of the motor with the healthy bearing has a normal distribution. The inner-race faulty bearing vibration has negative skewness, while the outer race faulty bearing has positive skewness with values close to zero. By looking at the

skewness values, it can be said that the distribution of vibration signals is symmetrical for all three cases. A similar analysis is also performed for other vibration axes and the results are also examined.

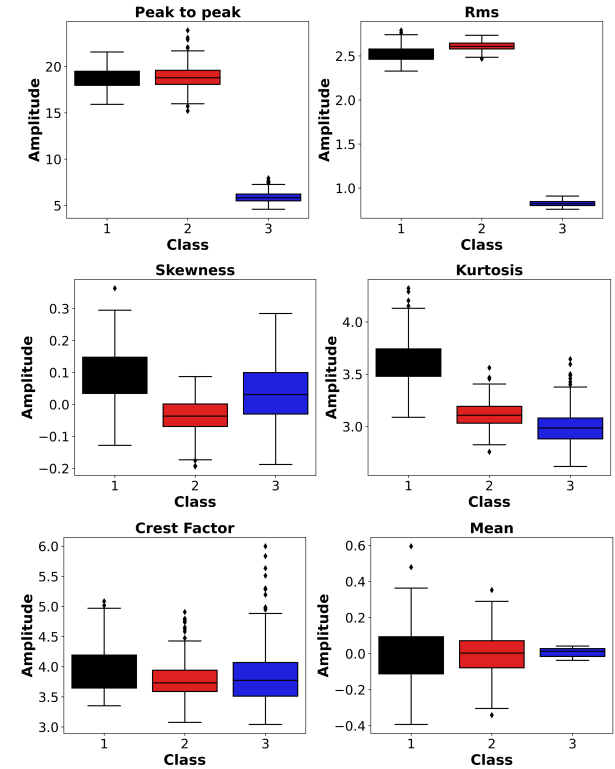


Fig. 6. Box plot representations of each statistical feature extracted from raw data belonging to the z vibrational axis

As one might observe from Fig. 6 plots, although it might be possible to distinguish healthy vs. faulty classes by solely examining some of the single-axis attribute values, detection among fault classes would not be possible. Therefore, other vibration axis features are examined closely. To obtain a self-learning data model that would not be susceptible to threshold and equipment drifts over time, machine learning algorithms are employed by incorporating other axes features as data attributes. For this, the x -axis, y -axis, and z -axis vibration signals are individually processed and supplied into k -NN and DT algorithms. Then dual combinations of axes signal with similar features (e.g., p2p values of both z and x -axis) are compared in terms of various model performance metrics.

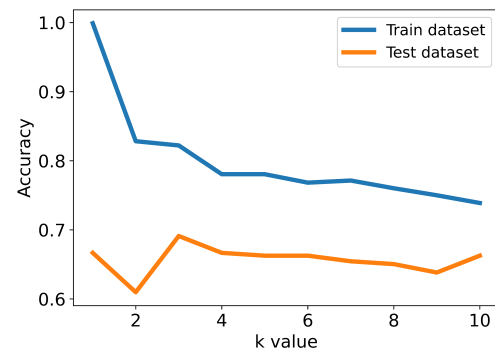


Fig. 7. Training and testing accuracy results for each randomly split data segment to determine the k parameter in the k -NN classifier model

To tune k -NN algorithm parameter k , iterative searching of k value is performed on a twofold randomly selected separate

dataset in each iteration called train and test. Classification tasks are performed for both train and test segments independently by varying the k value from 1 up to 10 as shown in Fig. 7. Since the k -NN algorithm makes a decision based on local information, selecting small values of k (e.g., $k = 1$) would make the model more susceptible to noise; therefore, $k = 3$ is selected.

Considering the performance and accuracy rate of the models based on the number of neighborhoods, the best model which can be used for the vibration data in this work can be selected as the model implemented with approximately 3 neighborhood values.

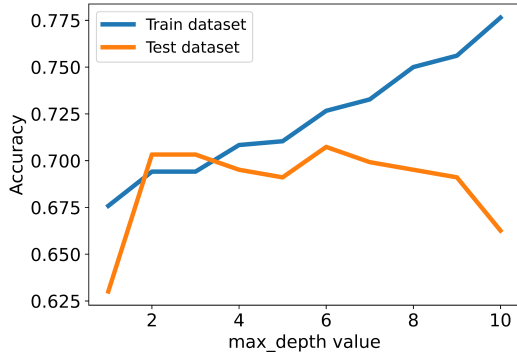


Fig. 8. Tuning maximum depth hyper-parameter value for DT classifier algorithm

The essential DT algorithm parameter to tune is the maximum depth that the tree will grow. For this, the DT algorithm is run iteratively for values ranging from 1 to 10 on the randomly selected train (80 %), test data (20 %) at each iteration, and the results are presented in Fig. 8. For training accuracy, as expected, while the maximum depth value increases, the training accuracy keeps increasing since the model starts learning the training data more. To avoid overfitting and to consider the accuracy results on the test data, a maximum depth value of four is determined as a reasonable value.

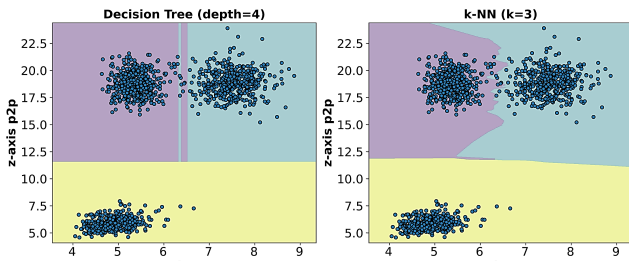


Fig. 9. Plots representing the decision boundaries obtained with tuned parameters for DT and k -NN classifier models

Fig. 9 presents an illustration of decision regions belonging to DT and k -NN models for z and y -axis p2p features when their corresponding tuned parameters are applied. It is evident that since the k -NN algorithm makes decisions locally based on the three nearest neighborhoods, it creates a rather more complex decision boundary than the DT model. As the DT model makes decisions on each node based on a single attribute, the decision boundary is created with rectilinear splits, which suit well considered a well-separated input feature space for our dataset.

A. Classification Model Performance

Confusion matrices obtained for k -NN and DT belonging to y and z -axis individually and combined yz axes on p2p features are presented in Fig. 10. and Fig. 11.



Fig. 10. Confusion matrices obtained with k -NN classifier belonging to data from y , z , and yz p2p features combined vibration axes

It is observed that p2p and rms features are among the most important statistical features for our experimental data; however, multiple axes along with the z -axis should be included to achieve successful classification performance. Note that similar results have also been obtained with the rms feature.

Fig. 11 presents the confusion matrix results obtained with the DT classifier on multiple axes with only p2p features. Similar results, up to 99.187 %, have also been observed. The obtained performance metrics results support the fact that the fault condition of the motor bearing (whether inner or outer race bearing fault) cannot be successfully identified by observing only a single axis vibration value.

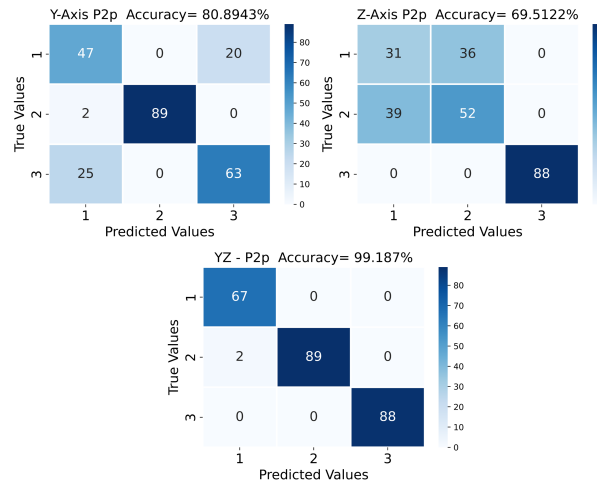


Fig. 11. Confusion matrices obtained with DT classifier belonging to data from y , z , and yz p2p features combined vibration axes

In Table I, model performance metrics with only the p2p feature belonging to the DT classifier are presented. These metrics include precision, recall, f1-score, and support values. As expected, combined yz axes results are significantly better as compared to the individual vibration axis.

TABLE I
DT MODEL PERFORMANCE METRICS OBSERVED VIA AXES ON P2P FEATURE VALUES

Vibration Axis		Precision	Recall	f1 score	Support
y	Outer race fault	0.64	0.70	0.67	67
	Inner race fault	1.00	0.98	0.99	91
	Healthy motor	0.76	0.72	0.74	88
z	Outer race fault	0.44	0.46	0.45	67
	Inner race fault	0.59	0.57	0.58	91
	Healthy motor	1.00	1.00	1.00	88
yz	Outer race fault	0.97	1.00	0.99	67
	Inner race fault	1.00	0.98	0.99	91
	Healthy motor	1.00	1.00	1.00	88

In Fig. 12 ROC (Receiver operating characteristic) and precision-recall curves obtained with the DT model on multiple axes p2p features are presented. To be able to demonstrate multi-class curves, the one-vs-all approach is utilized by employing DT models. Similar results have also been observed with k -NN models. In the plots, class 1 represents outer-race faulty bearing, class 2 represents inner-race faulty bearing, and class 3 represents healthy motor bearing data. In each graph, AUC (Area Under Curve) values are also presented for each class together with their micro and macro average values. As one can observe from the curves, the DT model can differentiate class 3 data easier than the other classes (especially on the z-axis); however, other classes' ROC and PR curve values transform into an ideal classifier model when multiple axes (y-z) are combined.

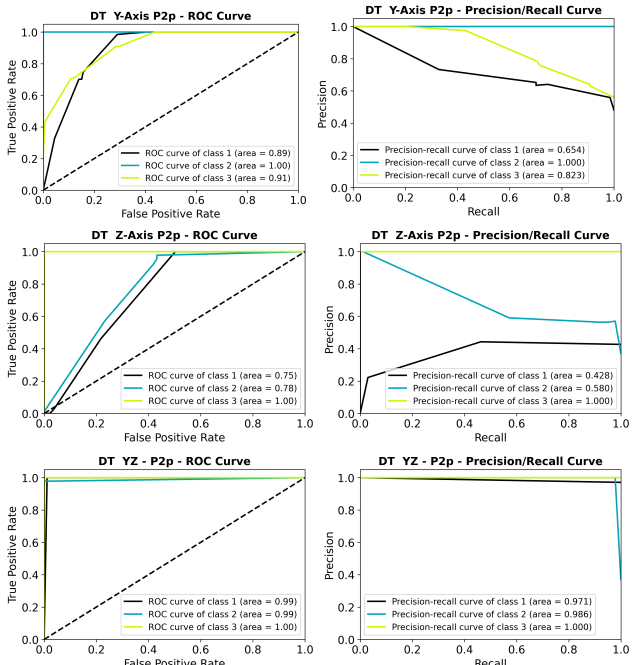


Fig. 12. ROC (Receiver operating characteristic) and PR (Precision-Recall) curves obtained with DT model utilizing P2P features on multiple axes

IV. DISCUSSIONS

When confusion matrices presented in Fig. 10 and Fig. 11 are analyzed, we can observe that both classifier algorithms can achieve similarly promising results on combined dual axes. This suggests that when descriptive statistics are observed for condition monitoring applications, single-axis vibrational data might be insufficient. Therefore, it is advised for researchers to use three-axis accelerometer sensors for vibration monitoring rather than single-axis.

When confusion matrices are analyzed, for both classification models, out of randomly selected 246 test data instances, 67 of them belong to the outer-race faulty class, 91 of them inner-face faulty class and 88 of them are healthy bearing data instances. In Fig. 10, with y -axis vibration data, k -NN correctly identifies 46 outer-race faults out of 67 and misclassifies 21 of them. Similarly, if k -NN had been used only on single-axis data for just the z -axis, misclassification rates would also be significantly high. This supports the benefit of multi-axes vibration analysis for fault detection and classification of motor bearing components.

V. CONCLUSIONS

This study focuses on condition monitoring of induction motor's bearing components, one of the most critical mechanical components for an induction motor. Considering the frequent breakdown of motors due to bearing parts and the impact on manufacturing due to unexpected downtimes, intelligent fault detection, and classification tasks are critical. Although vibration monitoring started being widespread in the industry, interpreting those collected signals usually requires expert knowledge and might not be readily available for field personnel. Furthermore, specific thresholding rule-based alarm generation approaches might not be sufficient since each motor might require different thresholding levels or machine characteristics might degrade, or vibration levels might drift over time. Therefore, with this study, descriptive statistics in the time domain are closely examined via experimentally generated fault-induced scenarios. Two simple machine learning algorithms are employed to obtain a self-learning data-driven decision model, and the results are examined in detail. Our experimental results show that for vibration monitoring, not all the descriptive statistics might be essential or sufficient enough to distinguish the health status of bearings, and out of the most important statistical features, multi-axes combinations should be employed. This study experimentally verified that it is possible to achieve nearly up to 100 % classification accuracies on induction motors' bearing fault detection and classification.

VI. REFERENCES

- [1] L. Frosini and E. Bassi, "Stator Current and Motor Efficiency as Indicators for Different Types of Bearing Faults in Induction Motors," *IEEE Transactions on Industrial Electronics*, vol. 57, no. 1, pp. 244-251, 2010, doi: 10.1109/tie.2009.2026770.
- [2] J. A.-D. Maeva Garcia, "Efficiency assessment of induction motors under different fault conditions," *IEEE Transactions on Industrial Electronics*, vol. 66, no. 10, pp. 8072-8081, 2018.
- [3] Z. Hosseinpoor, M. M. Arefi, R. Razavi-Far, N. Mozafari, and S. Hazbavi, "Virtual Sensors for Fault Diagnosis: A Case of Induction Motor Broken Rotor Bar," *IEEE Sensors Journal*, pp. 1-1, 2020, doi: 10.1109/jsen.2020.3033754.
- [4] O. Yaman, "An automated faults classification method based on binary pattern and neighborhood component analysis using induction motor," *Measurement*, vol. 168, p. 108323, 2021, doi: 10.1016/j.measurement.2020.108323.
- [5] H. Tang, S. Lu, G. Qian, J. Ding, Y. Liu, and Q. Wang, "IoT-Based Signal Enhancement and Compression Method for Efficient Motor Bearing Fault Diagnosis," *IEEE Sensors Journal*, vol. 21, no. 2, pp. 1820-1828, 2021, doi: 10.1109/jsen.2020.3017768.
- [6] L. Bin and V. C. Gungor, "Online and Remote Motor Energy Monitoring and Fault Diagnostics Using Wireless Sensor Networks," *IEEE Transactions on Industrial Electronics*, vol. 56, no. 11, pp. 4651-4659, 2009, doi: 10.1109/tie.2009.2028349.

- [7] D. T. Hoang and H. J. Kang, "A Motor Current Signal-Based Bearing Fault Diagnosis Using Deep Learning and Information Fusion," *IEEE Transactions on Instrumentation and Measurement*, vol. 69, no. 6, pp. 3325-3333, 2020, doi: 10.1109/tim.2019.2933119.
- [8] T. P. Carvalho, F. A. A. M. N. Soares, R. Vita, R. d. P. Francisco, J. P. Basto, and S. G. S. Alcalá, "A systematic literature review of machine learning methods applied to predictive maintenance," *Computers & Industrial Engineering*, vol. 137, p. 106024, 2019, doi: 10.1016/j.cie.2019.106024.
- [9] R. K. Molley, *Maintenance Fundamentals*, 2nd Edition ed. (Plant Engineering Maintenance Series). Elsevier Butterworth-Heinemann.
- [10] J. J. Montero Jimenez, S. Schwartz, R. Vingerhoeds, B. Grabot, and M. Salaün, "Towards multi-model approaches to predictive maintenance: A systematic literature survey on diagnostics and prognostics," *Journal of Manufacturing Systems*, vol. 56, pp. 539-557, 2020, doi: 10.1016/j.jmsy.2020.07.008.
- [11] Y. Merizalde, L. Hernández-Callejo, and O. Duque-Perez, "State of the Art and Trends in the Monitoring, Detection and Diagnosis of Failures in Electric Induction Motors," *Energies*, vol. 10, no. 7, p. 1056, 2017, doi: 10.3390/en10071056.
- [12] A. Choudhary, D. Goyal, S. L. Shimi, and A. Akula, "Condition Monitoring and Fault Diagnosis of Induction Motors: A Review," *Archives of Computational Methods in Engineering*, vol. 26, no. 4, pp. 1221-1238, 2018, doi: 10.1007/s11831-018-9286-z.
- [13] G. Yu, "A Concentrated Time-Frequency Analysis Tool for Bearing Fault Diagnosis," *IEEE Transactions on Instrumentation and Measurement*, vol. 69, no. 2, pp. 371-381, 2020, doi: 10.1109/tim.2019.2901514.
- [14] Z. Feng, M. Liang, and F. Chu, "Recent advances in time-frequency analysis methods for machinery fault diagnosis: A review with application examples," *Mechanical Systems and Signal Processing*, vol. 38, no. 1, pp. 165-205, 2013, doi: 10.1016/j.ymssp.2013.01.017.
- [15] T. Ishikawa, S. Shinagawa, and N. Kurita, "Analysis and Failure Diagnosis of Squirrel-Cage Induction Motor with Broken Rotor Bars and End Rings," *IEEJ Journal of Industry Applications*, vol. 2, no. 6, pp. 292-297, 2013, doi: 10.1541/ieejjia.2.292.
- [16] K. C. D. Komella, V. G. R. Mannam, and S. R. Rayapudi, "DWT based bearing fault detection in induction motor using noise cancellation," *Journal of Electrical Systems and Information Technology*, vol. 3, no. 3, pp. 411-427, 2016, doi: 10.1016/j.jesit.2016.07.002.
- [17] H. J. N. Dr. Mustafa M. Ibrahim, "Broken Bar Fault Detection Based on the Discrete Wavelet Transform and Artificial Neural Network," *Asian Transactions on Engineering*, vol. 03, no. 02.
- [18] G. Li, C. Deng, J. Wu, Z. Chen, and X. Xu, "Rolling Bearing Fault Diagnosis Based on Wavelet Packet Transform and Convolutional Neural Network," *Applied Sciences*, vol. 10, no. 3, p. 770, 2020, doi: 10.3390/app10030770.
- [19] D. Neupane and J. Seok, "Bearing Fault Detection and Diagnosis Using Case Western Reserve University Dataset With Deep Learning Approaches: A Review," *IEEE Access*, vol. 8, pp. 93155-93178, 2020, doi: 10.1109/access.2020.2990528.
- [20] M. Z. Ali, M. N. S. K. Shabbir, X. Liang, Y. Zhang, and T. Hu, "Machine Learning-Based Fault Diagnosis for Single- and Multi-Faults in Induction Motors Using Measured Stator Currents and Vibration Signals," *IEEE Transactions on Industry Applications*, vol. 55, no. 3, pp. 2378-2391, 2019, doi: 10.1109/tia.2019.2895797.
- [21] M. Sahraoui, A. Ghoggal, S. E. Zouzou, and M. E. Benbouzid, "Dynamic eccentricity in squirrel cage induction motors – Simulation and analytical study of its spectral signatures on stator currents," *Simulation Modelling Practice and Theory*, vol. 16, no. 9, pp. 1503-1513, 2008, doi: 10.1016/j.simpat.2008.08.007.
- [22] L. M. R. Baccarini, V. V. Rocha e Silva, B. R. de Menezes, and W. M. Caminhas, "SVM practical industrial application for mechanical faults diagnostic," *Expert Systems with Applications*, vol. 38, no. 6, pp. 6980-6984, 2011, doi: 10.1016/j.eswa.2010.12.017.
- [23] J. Lu, W. Qian, S. Li, and R. Cui, "Enhanced K-Nearest Neighbor for Intelligent Fault Diagnosis of Rotating Machinery," *Applied Sciences*, vol. 11, no. 3, 2021, doi: 10.3390/app11030919.
- [24] Y. Lei, B. Yang, X. Jiang, F. Jia, N. Li, and A. K. Nandi, "Applications of machine learning to machine fault diagnosis: A review and roadmap," *Mechanical Systems and Signal Processing*, vol. 138, 2020, doi: 10.1016/j.ymssp.2019.106587.
- [25] S.-w. Fei, "Fault Diagnosis of Bearing Based on Wavelet Packet Transform-Phase Space Reconstruction-Singular Value Decomposition and SVM Classifier," *Arabian Journal for Science and Engineering*, vol. 42, no. 5, pp. 1967-1975, 2017, doi: 10.1007/s13369-016-2406-x.
- [26] A. Bellini, F. Filippetti, C. Tassoni, and G. A. Capolino, "Advances in Diagnostic Techniques for Induction Machines," *IEEE Transactions on Industrial Electronics*, vol. 55, no. 12, pp. 4109-4126, 2008, doi: 10.1109/tie.2008.2007527.
- [27] R. E. Bearings. "Rolling Element Bearings or Anti-Friction Bearings." <https://www.brighthubengineering.com/machine-design/12886-rolling-element-bearings-or-anti-friction-bearings/> (accessed 26/05/2020).
- [28] A. S. Rajvardhan Jigyasu, Lini Mathew, Shantanu Chatterji, "Review of Condition Monitoring and Fault Diagnosis Methods for Induction Motor," *Proceedings of the Second International Conference on Intelligent Computing and Control Systems (ICICCS 2018)*, 2018.
- [29] G. Mittal, S. Patil, and A. Kumar Jalan, "A Review on Fault Diagnosis of Misaligned Rotor Systems," *International Journal of Perforability Engineering*, vol. 16, no. 4, p. 499, 2020, doi: 10.23940/ijpe.20.04.p1.499509.
- [30] A. A. Soofi and A. Awan, "Classification techniques in machine learning: applications and issues," *Journal of Basic and Applied Sciences*, vol. 13, pp. 459-465, 2017.

VII. BIOGRAPHIES

E. Irgat graduated from Gazi University, Technical Education Faculty of Electronics and Computer Education Department in Turkey in 1993 as summa cum laude and received his master's degree in Computer and Instructional Technologies at Anadolu University in Turkey in 2002. He is currently pursuing his doctorate at Kutahya Dumlupınar University Electrical and Electronics Engineering Department.

E. Cinar received his MSc. degree in 2010 from Rochester Institute of Technology, Rochester, NY in Electrical and Microelectronics Engineering as a Fulbright scholar and completed his Ph.D. studies at the same institution in 2015. After his doctoral studies, he has gained industrial experience and worked as Senior Engineer at GLOBALFOUNDRIES in Malta, NY as Advanced Process Control (APC), Fault Detection and Classification (FDC) engineer. In addition, he has worked as Senior Semiconductor Patterning Data Scientist at ASML-HMI in San Jose, CA. After being awarded an international fellowship for the Outstanding Researchers Program in Turkey, he has been working as a faculty member and Assistant Professor at Eskisehir Osmangazi University, Department of Computer Engineering in Turkey.

Dr. Eyup Cinar has multiple granted international patents, several journals, and conference publications, including awards given by international conference organizations.

A. Unsal received his MSc. degree in 1996 from Oklahoma State University, Stillwater, OK, in electrical engineering and Ph.D. degree in 2001 from Oregon State University, Corvallis, OR in electrical engineering. After completing his Ph.D. degree, he joined Kutahya Dumlupınar University as an Assistant Professor at the Department of Electrical and Electronics Engineering. He was promoted to the rank of Associate Professor in 2014. He has been working as a Professor in the same department since 2019. His current research interests include power electronics, active filters, fault diagnosis, and electric machines.